Article

Research on Hybrid Heating System in Cold Oilfield Regions

Meng Xu [1], Zhiyang Xu [2,3], Xinxin Wei [2,3], Gaoxiang Zhang [2,3] and Changyu Liu [2,3,*]

1 Resource Engineering College of Heilongjiang University of Technology, Heping Street, Jixi 158100, China; nepuxm@126.com
2 School of Architecture and Civil Engineering, Northeast Petroleum University, Fazhan Lu Street, Daqing 163318, China; xuzhiyang15242949935@163.com (Z.X.); 15194903502@163.com (X.W.); zgx046710@163.com (G.Z.)
3 International Joint Laboratory on Low-Carbon and New-Energy Nexus, Northeast Petroleum University, Daqing 163318, China
* Correspondence: lcy57649976@163.com

Abstract: Efficient and clean treatment of wastewater and energy recovery and utilization are important links to realize low-carbon development of oilfields. Therefore, this paper innovatively proposes a multi-energy complementary co-production heating system which fully and efficiently utilizes solar energy resources, oilfield waste heat resources, and biomass resources. At the same time, a typical dormitory building in the oil region was selected as the research object, the system equipment selection was calculated according to the relevant design specifications. On this basis, the simulation system model is established, and the evaluation index and operation control strategy suitable for the system are proposed. The energy utilization rate of the system and the economic, energy-saving, and environmental benefits of the system are simulated. The results show that, under the simulated conditions of two typical days and a heating season, the main heat load of the system is borne by the sewage source heat pump, the energy efficiency is relatively low in the cold period, and the energy-saving characteristics are not obvious. With the increase in heating temperature and anaerobic reactor volume, the energy consumption of the system also increases, and the energy efficiency ratio of each subsystem and the comprehensive energy efficiency ratio of the system gradually decrease. In addition, although the initial investment in cogeneration heating systems is high, the operating costs and environmental benefits are huge. Under the condition of maintaining 35 °C, the anaerobic reactor in the system can reduce carbon emissions by 12.15 t per year, reduce sulfur dioxide emissions by 98.4 kg, reduce dust emissions by 49.2 kg, and treat up to 2700 t of sewage per year, which has broad application prospects.

Keywords: direct suction solar anaerobic reactor; sewage source heat pump; TRNSYS simulation; combined heating system

1. Introduction

With the continuous development of the global economy and the improvement of people's living standards, the energy consumption in the construction field is increasing [1]. The massive consumption of energy has raised concerns about the exhaustion of energy resources. Therefore, people began to pay more attention to the research, development, and utilization of non-polluting new and renewable energy, including solar energy, geothermal energy, wind energy, ocean energy, and biological energy [2], focusing on exploring how to use different types of energy in a comprehensive way [3]. This comprehensive utilization method aims to eliminate the adverse factors that may be brought about by single-energy utilization [4] and give full play to the unique advantages of each energy to improve the overall energy utilization efficiency [5]. This also includes integrated utilization options tailored to local resources to promote the development and utilization of new and renewable energy sources to meet growing energy demand and reduce dependence on traditional energy sources [6].

1.1. Research on Combined Heating System

In areas rich in solar energy resources, Chen Yaowen et al. proposed a centralized solar energy and biogas mixed heating system to meet the needs of rural areas and improve the stability and economy of the system heating. The economic feasibility of the combined heating system is better than that of the traditional single solar heating system, and the investment payback period can be shortened by about 50% [7]. Long research teams proposed a composite heating system combining solar hot water and an air source heat pump to achieve a variety of heating methods of combined heating, including parallel, series, and other connection methods. In the cold season, through simulation analysis, it was found that solar radiation and ambient temperature have important effects on energy efficiency, especially in cold climates. The combined application of solar energy and air source heat pumps is expected to improve the performance of heating systems [8]. Yang Weibo et al. conducted an in-depth study on the different coupling modes of solar ground source heat pump systems installed in buildings in Nanjing. The results show that the heating load ratios of solar energy and geothermal energy are 43.3% and 50.2%, respectively, when the system is operated day and night. During the day, solar collectors collect excess heat and store it in the soil for end-use heating at night. This operation mode effectively improves the efficiency of the collector and realizes the efficient coupling of solar energy and geothermal energy [9]. Huan, C proposed a combined solar-assisted heat pump system with two modes of operation, series and parallel. The research team performed performance tests on the system using TRNSYS 18_1 software. The results show that the system has excellent performance in energy saving [10]. In an area rich in geothermal resources, Wang Yubo et al. studied the feasibility of the air-ground source heat pump coupled energy storage system and calculated that, compared with the traditional ground source heat pump system, the annual operating cost of the new system is only 58% of that of the traditional system, and the carbon emission can be reduced by 7.14%, which has good economic and environmental benefits [11]. Zhang Congguang et al. conducted an experimental study on the thermal performance of the combined solar energy and ground source heat pump system of a single-family residence, focusing on the dynamic thermal behavior of the heat accumulator under different working conditions, and the results verified the operational reliability and good economic and environmental benefits of the combined system [12]. In the oilfield area, there is a large amount of waste heat resources to be used, which attracts domestic and foreign scholars to study it [13]. Zhu et al. proposed an innovative heating system that uses oil production water as a heat source. The system is unique in that it not only meets the heating needs of the building, but also effectively reduces the consumption of fossil fuels and reduces carbon dioxide emissions. By utilizing these wastewater waste heat resources, energy costs are reduced and dependence on traditional energy sources is reduced. In addition, such heating systems help to reduce adverse environmental impacts and promote sustainable development. Therefore, the utilization of waste heat from oilfield wastewater has great potential in the field of heating, which is worthy of further study and application [14].

Chatz istougianni, N et al. proved through experimental studies that biomass can be used as a heat source to support small-scale central heating systems, especially for public buildings. This study provides practical demonstration and support for the application of biomass energy in heating system [15]. Our research team, including Tian Yishui and other scholars, conducted research on solar energy and biomass energy combined heating system, proposed a design scheme, and established an economic analysis model. The results show that this system can make full use of the advantages of biomass energy and solar energy, extend the service life of biomass pellet burners, and make up for the shortcomings of solar energy instability. It is highly complementary. This research provides a new idea and scheme for the joint application of renewable energy [16].

1.2. Advantages of Co-Generation Heating System

The above studies show that the comprehensive use of clean and renewable energy according to local conditions can eliminate the disadvantages of single energy use. As with areas rich in solar energy resources, solar heating has shortcomings such as intermittency and instability [13]. Combining solar energy with other heating systems can offer a variety of benefits. First, this combination can enhance the stability and reliability of the heating system so that the solar system and other heating systems complement each other. When the solar system cannot meet the heating demand, other systems can step in to ensure continuous heating. Secondly, this combination can also improve heating efficiency and reduce energy consumption. Solar energy can provide heat during the day and be stored for use at night or on cloudy days. This can improve the energy efficiency of the heating system and reduce the dependence on traditional energy sources [17]. In areas rich in geothermal resources, ground source heat pumps may be affected by the external environment, and the combination of ground source heat pumps and other heating systems can make up for this, which can ensure the heating needs of users and is a wise and effective way to provide stable, efficient, and sustainable heating solutions [18]. The waste heat resources of oilfields are rich, so it is considered to use the abundant waste heat resources of oilfields to supply heat and reduce the thermal pollution caused by its direct emission to the environment [19], as well as to reduce the consumption of fossil fuels [20].

1.3. Problems Faced by Combined Heating Systems

The authors presented comprehensive performance results of an experimental PV-T system using microencapsulated phase change material slurry as the cooling medium [21]. A renewable energy source is a source that, in the process of energy production, uses wind energy; solar radiation; geothermal energy; waves; sea currents and tides; fall of rivers; and energy obtained from biomass, biogas from landfill, or from the process of anaerobic digestion of sewage sludge [22]. In most cases, solar energy is used to produce clean thermal or electrical energy in well-known dedicated devices, namely, solar thermal collectors and photovoltaic panels (PV) [23]. A certain degree of matching between the electricity consumption and production profiles can be advantageous to the building's and electricity grid's performance and economy, as will be demonstrated in the current study [24]. This hybrid system includes small-scale pellet boilers and small-dimension parabolic trough solar collectors (PTC), which is the first small-sized PTC facility proposed for low-temperature applications (less than 100 °C) in Morocco [25].

1.4. Research Content of This Paper

Based on the research of the above scholars and the unique natural resources of the Daqing region, this paper also considers the national policy of clean energy application. To reduce environmental pollution and improve energy utilization efficiency while making full use of oilfield sewage waste heat, as well as to solve the problem of environmental pollution and improve the energy efficiency of the system, this study proposes a multi-energy complementary combined heating system that comprehensively utilizes solar energy resources, oilfield waste heat resources, and biomass resources, aiming to achieve efficient and clean treatment of oilfield sewage and energy recovery and utilization.

In this paper, a typical dormitory apartment building in the oil region was selected as the research object by combining theoretical analysis with numerical simulation calculation. DeST-Design Environment Simulation Toolkit was used to simulate the building heat load, put forward the indicators suitable for system evaluation, set up the simulation system model, and simulate the system operation performance based on TRNSYS software. The model is verified and analyzed to ensure accuracy and reliability. The operation control strategy of the multi-energy complementary combined heating system is proposed. The energy utilization and operation performance of the system are analyzed and calculated using the simulation model, and the economic, energy-saving, and environmental benefits of the system are simulated and calculated.

1.5. The Innovative Aspect of This Paper

Based on the above studies, we found that the utilization and treatment of oilfield wastewater has great potential; however, the current research on multi-energy complementary systems has not achieved a coupled solution for their heat and mass transfer. Accordingly, the novelty of this study lies in the proposal of a new hybrid heating system that combines anaerobic reaction technology and solar energy technology to address the large amount of high-ammonia nitrogen dry distillation wastewater contained in shale oil in the Daqing Oilfield area, which can be applied to typical dormitory buildings in the region. This system not only achieves multi-energy complementarity, but also reduces environmental pollution.

2. System Introduction

The multi-energy complementary combined heating system can utilize solar energy, sewage heat energy, and biomass energy at the same time; reduce heating costs and pollutant emissions; and have good social and economic benefits. A schematic diagram of the multi-energy complementary combined heating system is shown in Figure 1. The working process of each subsystem in the combined heating system is shown, including the anaerobic reactor biogas boiler subsystem, where sewage enters the direct absorption solar anaerobic reactor and ferments biogas together with the stalks filled in the reactor. The resulting biogas is burned in a biogas boiler for heating. The sewage source heat pump subsystem works as follows: Sewage flows through the countercurrent plate heat exchanger for heat exchange, the heat exchanger in the working medium absorbs heat, and then the sewage flows into the sewage source heat pump system for heating. Both subsystems are connected to heat storage tanks. When the heat generated by the system is greater than the building load, the excess heat will be stored, and when the heat is insufficient, it will be heated.
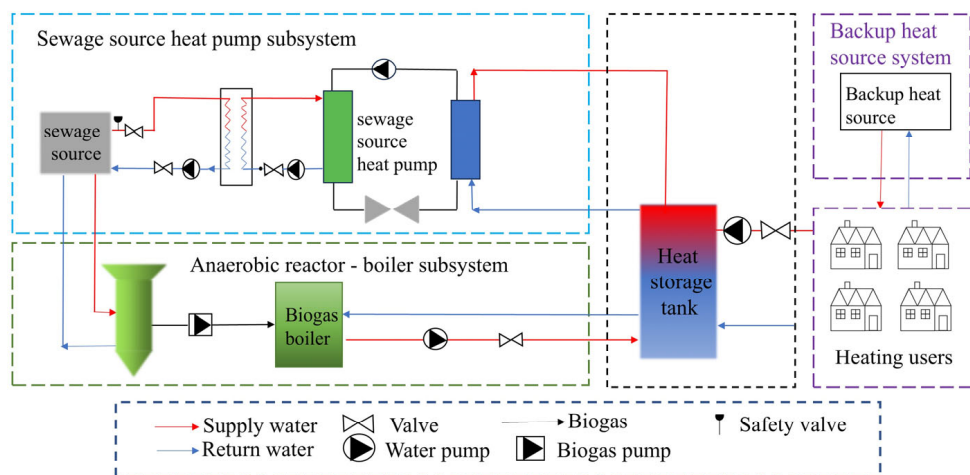

Figure 1. Schematic diagram of multi-energy complementary combined heating system.

By monitoring the temperature of the outlet water temperature of each heating subsystem, the opening and closing of the valve are controlled to control the system's heating. In the treatment and utilization process of oilfield sewage, oilfield sewage must be treated before it can be discharged. In this study, the anaerobic reactor subsystem is always kept open to treat sewage, and the biogas generated in the process is burned for building heating. A 3D drawing of the proposed building is shown in Figure 2.
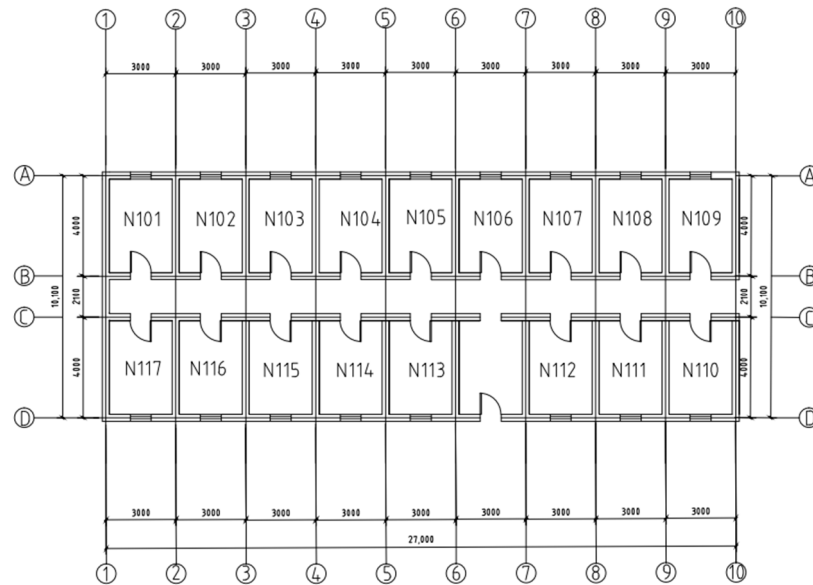
Figure 2. Building floor plan.

3. System Mathematical Model

3.1. Mathematical Model of Components

1. Sewage source heat pump unit

Calculation of key parameters of sewage source heat pump: The heat produced by the heat pump unit is [26]:

$$Q_{heating} = Q_{absorbed} + P_{heating} \tag{1}$$

$Q_{heating}$: sewage source heat pump heat production, kW; $Q_{absorbed}$: heat pumps absorb heat, kW; $P_{heating}$: the power consumption of sewage source heat pump, kW.

The sewage source heat pump COP is shown as follows:

$$COP_{sew} = \frac{Q_{heating}}{P_{heating}} \tag{2}$$

3.2. Anaerobic Reactor

In order to ensure the continuity of gas production in the biogas digester, the anaerobic reactor should be kept at a constant temperature as much as possible. In order to keep the biogas tank at a constant temperature, the reactor needs to be heated.

Heat required for anaerobic reactor insulation:

$$Q_{AD,ioz} = (Q_{f,r} + Q_{f,f} + Q_{f,w}) \times 10^{-3} = [(A_r K_r + A_f K_f + A_{ws} K_{ws})(T - T_a)] \times 10^{-3} \tag{3}$$

$Q_{f,r}$ represents the heat loss at the top of the anaerobic reactor, kW; $Q_{f,ft}$ represents the heat loss at the bottom of the anaerobic reactor, kW; $Q_{f,w}$ represents the heat loss of the side wall of the anaerobic reactor, kW; K_r represents the average heat transfer coefficient at the top of the anaerobic reactor, W/(m^2·K); A_r represents the area at the top of the anaerobic reactor, m^2; K_f represents the average heat transfer coefficient at the bottom of the anaerobic reactor, W/(m^2·K); A_f represents the area at the top of the anaerobic reactor, m^2; K_f represents the heat transfer coefficient between the feed liquid and the side wall of the anaerobic reactor, W/(m^2·K); and A_{ws} represents the side wall area where the feed liquid inside the anaerobic reactor is in contact with the tank wall, m^2.

3.3. Biogas Boiler

The thermometer formula for setting the outlet water temperature is as follows:

$$t_{out} = t_{in} + \frac{Q_{fluid}}{cm} \tag{4}$$

T_{out} denotes the temperature of the boiler water, °C; t_{in} represents the boiler water temperature, °C; Q_{fluid} represents the actual heat produced by the boiler, kW; c represents the specific heat capacity of water, kJ/(kg·°C); and m represents the boiler water flow, kg/s.

Biogas boiler combustion The biogas produced by the anaerobic reactor generates thermal energy, which is transferred to the heat medium flowing through the boiler heat exchange tube through combustion. The energy balance equation of the biogas boiler is as follows:

$$q_{Bb} = q_{Bb,h} + q_{Bb,loss} \tag{5}$$

q_{Bb} represents the heat released by the biogas boiler burning biogas, kW; $q_{Bb,h}$ represents the effective heat output of the biogas boiler, kW; and $q_{Bb,loss}$ represents the heat lost during the operation of the biogas boiler, kW.

Heat output of biogas boiler [27]:

$$q_{Bb,h} = \eta_{Bb} v_{Bb} R_{bg} \tag{6}$$

η_{Bb} represents the thermal efficiency of the biogas boiler, %; v_{Bb} represents the amount of methane consumed by the biogas boiler, m³; and R_{bg} represents the biogas calorific value, kJ/m³.

3.4. Heat Storage Tank

The energy balance equation of the heat storage tank is [28]:

$$q_{tank} = q_{sew,a} + q_{Bb,h} - q_{load} - q_{tank,loss} \tag{7}$$

$$q_{load} = q_{bio,h} + q_{sew,h} \tag{8}$$

$$q_{tank,loss} = UA(T_{tank} - T_a) \tag{9}$$

Q_{tank} represents the remaining heat in the hot water tank, kW; q_{load} represents the heat provided to the user by the heat storage tank, kW; $q_{tank,loss}$ represents the heat loss of the heat storage tank, kW; T_{tank} represents the average temperature of the water in the storage tank, °C; U represents the heat transfer coefficient of the heat storage tank box, W/(m²·°C); and A represents the heat transfer area of the heat storage tank, m².

3.5. Controller

The system uses temperature changes to control the start and stop of components in the system during operation. The mathematical description of this component is as follows.

When the controller is set to off at the previous moment:

$$If\ \gamma_i = 1\ and\ \Delta T_L \leq (T_H - T_L), \gamma_0 = 1 \tag{10}$$

$$If\ \gamma_i = 1\ and\ \Delta T_L \leq (T_H - T_L), \gamma_0 = 0 \tag{11}$$

When the controller is set to on at the previous time:

$$If\ \gamma_i = 0\ and\ \Delta T_H \leq (T_H - T_L), \gamma_0 = 1 \tag{12}$$

$$If\ \gamma_i = 0\ and\ \Delta T_H > (T_H - T_L), \gamma_0 = 0 \tag{13}$$

T_H, T_L represent the upper and lower limits of temperature, °C; ΔT_H, ΔT_L represent the dead zone temperature difference, °C; γ_i represents the output signal of Type2b at the

previous time; γ_0 represents the present-time output signal; and Output "0" means off, while output "1" means on.

3.6. System Evaluation Index

In the complementary coupled energy supply system, the anaerobic reactor boiler subsystem consumes heat and produces biogas energy, so it is both a "consumer" and a "producer". The less heat consumed by the anaerobic reactor-boiler subsystem and the more energy generated, the better the performance of the anaerobic reactor boiler subsystem. A new energy efficiency index, EEF (energy efficiency of anaerobic reactor biogas boiler system), that is, the ratio of heat supply to heat demand of the biogas boiler subsystem of the anaerobic reactor, is defined to describe the performance of the biogas boiler subsystem of the anaerobic reactor. The defined equation is as follows:

$$EEF_{bio} = \frac{q_{Bb,h}}{q_{sew,bh}} \tag{14}$$

3.7. The Coefficient of Performance of Wastewater Source Heat Pump System

$$COP_{sew} = \frac{q_{sew,h} + q_{sew,bh}}{P_{sew,h} + P_{sew,bh}} \tag{15}$$

$P_{sew,c}$ denotes the input power of the wastewater source heat pump system for the building heating process; $P_{sew,bc}$ represents the input power of the wastewater source heat pump system to the anaerobic reactor biogas boiler system.

3.8. The Performance Coefficient of the WHBCHS

$$COP_{sys} = \frac{q_{bio,h} + q_{sew,h} + q_{sew,bh}}{P_{bio,c} + P_{sew,c} + P_{sew,bc}} \tag{16}$$

$p_{bio,c}$ represents the input power of the biogas boiler system of the anaerobic reactor to the building-heating process.

3.9. WHBCHS Correlation

$$REL_{sys} = EEF_{bio} \times COP_{sew} \tag{17}$$

3.10. The Annual Cost of Combined Heating System Is Calculated by the Following Formula

$$f(x) = \frac{i(1+i)^m}{(1+i)^m - 1} \times C_0 + Price \times W_{all} \tag{18}$$

$f(x)$ represents the annual cost value, CNY; C_0 represents the initial investment in the system, CNY; i represents the annual interest rate of bank loans, 6.9%; W_{all} represents the total system energy consumption, kWh; *Price* represents the local electricity prices, 0.5 CNY/kW; and m represents the system's service life.

Carbon dioxide emission reduction can be calculated as follows:

$$Q_{co_2} = Q_s \times V_{co_2} \tag{19}$$

Q_{co_2} represents the carbon dioxide reduction, kg; V_{co_2} represents the carbon dioxide emission factor of standard coal, which is 2.47 kg/kgce.

Sulfur dioxide emission reduction:

$$Q_{so_2} = Q_s \times V_{so_2} \tag{20}$$

Q_{so_2} represents the sulfur dioxide emission reduction, kg; V_{so_2} represents the sulfur dioxide emission factor of standard coal, which is 0.02 kg/kgce.

Dust reduction:

$$Q_{fc} = Q_s \times V_{fc} \tag{21}$$

Q_{fc} represents the dust reduction for multi-energy complementary combined heating systems, kg; V_{fc} represents the dust emission factor of standard coal, which is 0.01 kg/kgce.

4. Energy Simulation Results

4.1. Calculation of Building Heat Load

A dormitory apartment building in Youqu District of Daqing City is taken as the research object. The dormitory apartment is a three-storey building with a heating area of 1364 m², which was simulated using DeST simulation software as shown in the Tables 1 and 2.

Table 1. Structural parameters of dormitory apartments in oil area.

Enclosure Structure	Building Structure
Outer wall	20 mm cement mortar +120 mm expanded benzene board +20 mm cement mortar; 490 mm clay brick building
Interior wall	10 mm cement mortar +120 mm clay brick +10 mm cement mortar
roof	20 mm color steel plate +20 mm asphalt felt +100 mm reinforced concrete building +100 mm polystyrene board
window	5 mm flat glass +9 mm air +5 mm flat glass
Outer door	70 mm double metal insulation
Interior door	50 mm single wooden door

Table 2. Statistics of building heat load.

Statistical Item	Maximum Heat Load/kW During Heating Season	Average Heat Load/kW During Heating Season	Cumulative Heat Load/kW During Heating Season
Statistical value	61.63	37.25	156,768

4.2. Construction of Heating System Simulation Platform

#### 4.2.1. Construction of Simulation Model

TRNSYS is a professional building energy analysis and system simulation software. TRNSYS has a rich library of components, and users can choose the appropriate components according to their needs [29]. Performance evaluation and system optimization can be performed, including the prediction of energy consumption, temperature, humidity, wind speed, and other parameters, and TRNSYS can be used to optimize the design and operation of energy systems to maximize energy efficiency and reduce costs [30]. Li Hong et al. used TRNSYS to conduct simulation research on the solar heat pump combined heating system and discussed the influence of the main parameters on the system's performance [31]. Wang Dengjia et al. used TRNSYS to optimize and economically analyze the combined system of a biogas boiler and solar heating [32]. However, the above studies were all based on the built-in modules of TRNSYS for modeling and simulation, while in this study, the anaerobic reactor has no corresponding fixed module in TRNSYS, and its gas production process is affected by various factors. Therefore, this paper aims to study the gas production of anaerobic reactors based on the general-purpose and inclusive model developed by the International Water Association (IWA), which is mostly used in the current research on the biochemical process of anaerobic fermentation. It can better analyze the anaerobic digestion model No. 1 (ADM1) of biogas production, fit the gas production curve according to the gas production results, and compile and simulate in TRNSYS [33,34].

We selected corresponding modules on the TRNSYS software platform to connect to the system based on the system principles. Table 3 lists the modules used in the system.

Table 3. Multi-energy complementary combined heating system modules.

Assembly Unit	Module
Type15-2	Meteorological file reading
Type668	Sewage source heat pump unit
Type700	Biogas boiler
Type4c	Heat storage tank
Type649	Manifold valve
Type577	Sewage temperature
Typel14	Circulating water pump
Type682	Building heat load
Type5	Heat exchanger
Type14h	Time controller
Type2b	Temperature difference controller
Type24	Numerical integrator
Type9e	Load file
Type65c	Operation result output
Type147	Anaerobic reactor

The simulation model of the heating system is built according to the multi-energy complementary joint heating system and the control logic. The simulation model of the multi-energy complementary joint heating system is shown in Figure 3.
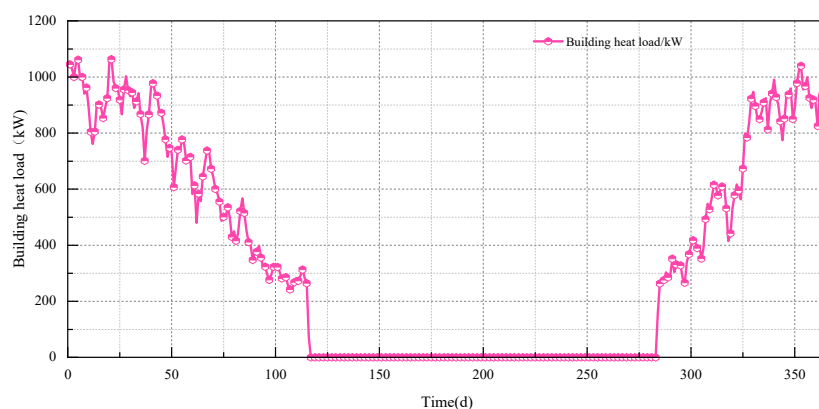
Figure 3. Annual heat load of the building.

4.2.2. System Control Policy

In this study, TRNSYS software was used to simulate the multi-energy complementary combined heating system, and the simulation model was established. The control strategy of the multi-energy complementary combined heating system is as follows:

In this study, the biogas boiler subsystem of the anaerobic reactor is controlled by temperature difference, and the temperature difference between the effluent temperature of the boiler and the internal temperature of the heat storage tank is monitored. We set the upper limit of temperature difference to 5 °C and the lower limit of temperature difference to 2 °C shown in the Figure 4. When the temperature was higher than the upper limit of temperature difference, the heat collection circulation pump was open. When the temperature was lower than the lower limit, the heat-collecting circulating pump was closed. In addition, in order to prevent the water supply of the heat storage tank from overheating, when the temperature in the water tank exceeded 60 °C, the two sub-system side circulation pumps stopped running regardless of the temperature difference. The logic control diagram of the system is shown in Figure 5 below.
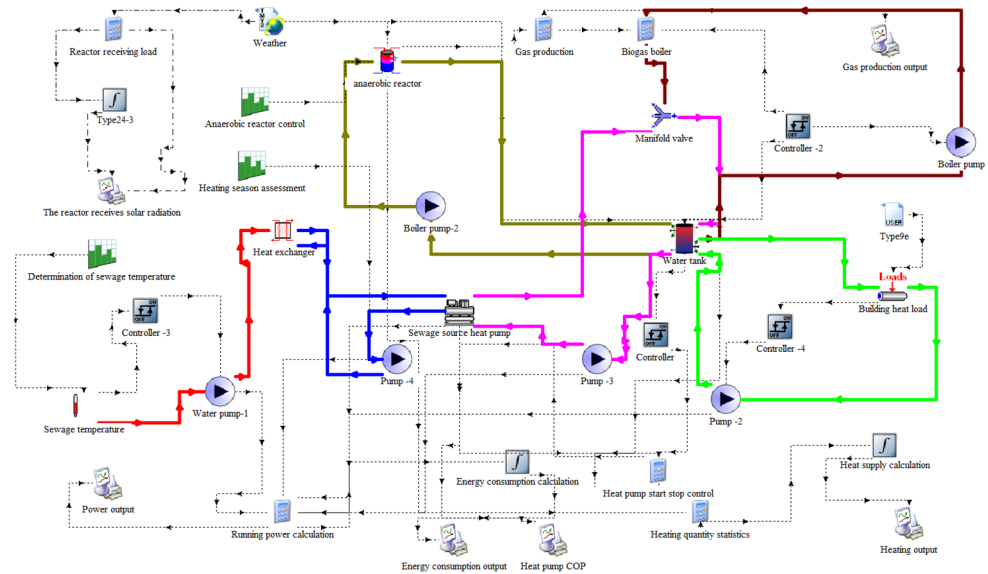
Figure 4. Simulation model of multi-energy complementary combined heating system.
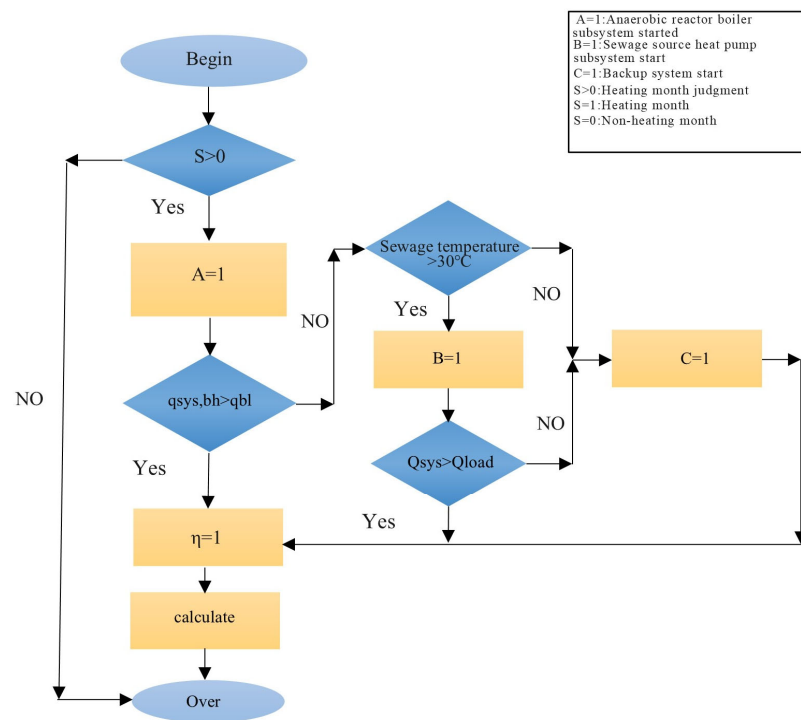

Figure 5. Logic control strategy.

The control of the sewage source heat pump subsystem is controlled according to the internal temperature of the heat storage tank. When the outlet temperature of the heat storage tank is lower than 40 °C, the heat pump is in the open state; when the outlet water temperature is higher than 40 °C, the heat pump is in the closed state.

4.2.3. Model Verification

TRNSYS software was used for simulation in this simulation. In order to prove the reliability of the model and verify the model, the experimental model of Jiang Mingzhi was used for this verification, and the same conditions were set in the model as Jiang Mingzhi's experiment [21]. We verified the reliability of the model proposed in this study. The simulation value of water supply and the return temperature of the sewage source

heat pump unit were compared with the experimental value, and the variance between the experimental result and the simulated value was evaluated by ARE and RMSE. According to Figures 6 and 7, it can be seen that under the conditions of the coldest day, the heat supply of the biogas boiler subsystem of the anaerobic reactor is small, while the heat load required by the building is large, and the sewage source heat pump bears most of the heating heat load. During the transition days, the heat supply of the biogas boiler subsystem of the anaerobic reactor increased by 10.9% per hour compared with the average hour of the coldest day, and the heat supply of the sewage source heat pump subsystem decreased. Figure 6 shows the hourly variation curve of the building heat load on the coldest day and the transition day. It can be seen that the building heat load on the coldest day is always greater than that on the transition day. The hourly heat load of the buildings on the coldest day is more than 35 kW, and the maximum value is 49.36 kW, while the hourly heat load of the buildings on the transition day is less than 30 kW, and the minimum value is only 18.46 kW. Figure 7 is the hourly variation diagram of the heat supply of the biogas boiler subsystem of the anaerobic reactor. These formulas were calculated as follows:

$$\text{ARE} = \frac{1}{n}\sum_{i=1}^{n}\frac{|s_i - e_i|}{e_i} \times 100\% \tag{22}$$

$$\text{RMSE} = \sqrt{\frac{1}{n}\sum_{i=1}^{n}(s_i - e_i)^2} \tag{23}$$
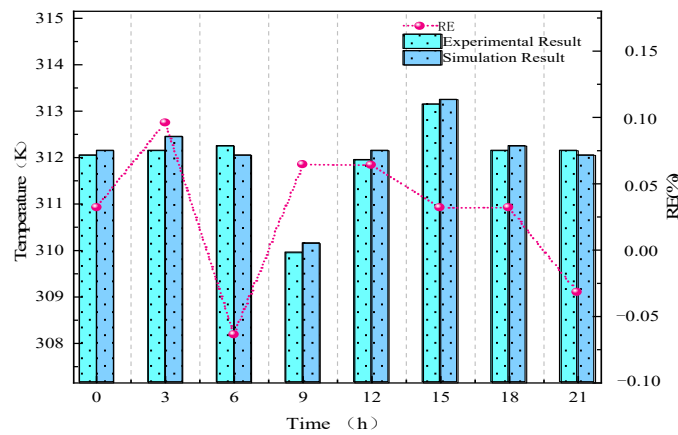

Figure 6. Sewage source heat pump unit water temperature experiments compared with the simulation data.
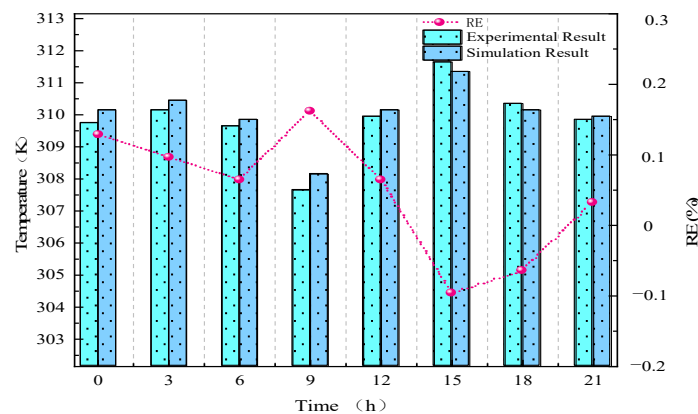

Figure 7. Comparison of experimental and simulation data of return water temperature of sewage source heat pump unit.

According to the information, it can be calculated that the ARE and RMSE of the supply water temperature are 0.418% and 0.18 K, respectively, and the ARE and RMSE of the return water temperature are 0.75% and 0.3 K, respectively. This shows that there is a strong correlation between the experimental data and the simulation data, so the reliability and accuracy of the simulation results can be ensured by using this model, which can be used for the subsequent modeling and analysis of the combined heating system.

5. Discussion of Results

5.1. Simulation Operation Analysis of Typical Daytime Combined Heating System

It can be seen from the diagram that the heat supply of the biogas boiler subsystem of the anaerobic reactor changes in a wavy trend of first decreasing, then increasing, and then gradually decreasing within a day. The peak value of the heat supply of the biogas boiler subsystem of the anaerobic reactor appears at around 18:00, which is due to the influence of solar irradiation. Around 10:00, the solar irradiance gradually increases, the direct absorption solar anaerobic reactor absorbs solar radiation, the reaction liquid temperature in the reactor rises, the gas production in the reactor gradually increases, and the corresponding biogas boiler subsystem of the anaerobic reactor increases the heat supply. With the gradual increase in solar radiation, the reaction liquid temperature in the reactor also keeps rising. When the temperature is 18, the gas production of the reactor is the largest, and the heat supply of the biogas boiler subsystem of the anaerobic reactor is also the largest. The amount of heating provided by the biogas boiler subsystem of the anaerobic reactor is always smaller than that on the transition day on the coldest day. Since the outdoor temperature and solar irradiation intensity are lower than that on the transition day on the coldest day, the anaerobic reactor not only obtains lower solar radiation intensity, but also emits more heat under lower environmental conditions, so the reactor temperature is lower and the gas production is smaller. Correspondingly, less heat is provided. Figure 8 shows the variation curves of the comprehensive energy efficiency ratio of the system and the energy efficiency ratio of the heat pump for the multi-energy complementary combined heating system during the annual heating season. Under different water supply temperatures, the energy efficiency ratio simulation results of sewage source heat pump subsystem are shown in Figure 9.

The simulation operation data of the combined heating system on two typical days are shown in Table 4. As can be seen from Table 4, under the conditions of two typical days, the sewage source heat pump bore most of the heating load, and the comprehensive energy efficiency ratios of the system were only 1.61 on the coldest day and 2.54 on the transition day.
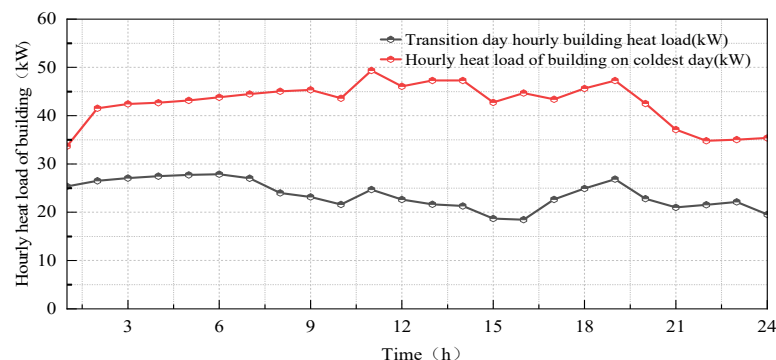

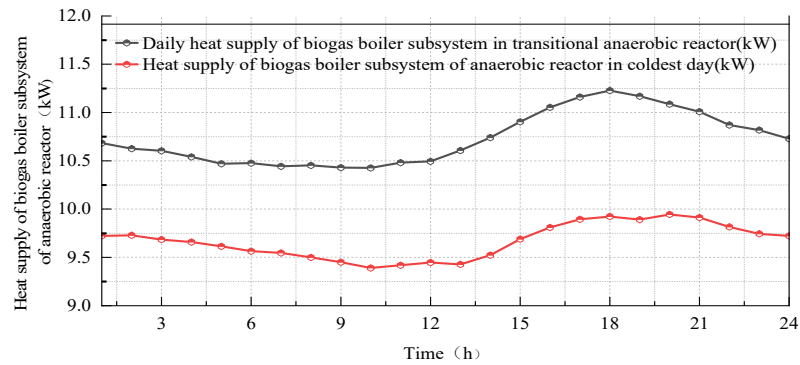**Figure 8.** Hourly thermal loads of buildings under two typical daily conditions.

Figure 9. Heat supply of biogas boiler subsystem of anaerobic reactor under two typical daily conditions.

Table 4. Simulation operation data of heating system on two typical days.

Item	Coldest Day Transition Day	Coldest Day Transition Day
Sewage source heat pump system cumulative heat supply (kWh)	792.48	309.33
Cumulative heat supply of anaerobic reactor biogas boiler system (kWh)	232.02	257.50
Total system energy consumption (kWh)	633.27	423.11
COP_{sys}	1.61	2.54

5.2. System Heating Season Simulation Operation Analysis

Simulation analysis of the annual heating season of the combined heating system was carried out, in which the heating season lasted from 1 January to 20 April and from 20 October to 31 December. In the operating cycle of the annual heating season, the cumulative heat supply of the sewage source heat pump subsystem, the cumulative heat supply of the anaerobic reactor biogas boiler subsystem, and the total energy consumption of the system are shown in Table 5. It can be seen that, in the multi-energy complementary combined heating system, the main heating load was borne by the sewage source heat pump. The cumulative heat supply of the anaerobic reactor biogas boiler system was only 42,500 kWh, and the heat supply was only 24.8% of the whole system. The total energy consumption of the combined system during the heating season was 107,557 kWh.

Table 5. System heating season operation simulation data statistics.

Item	Multi-Energy Complementary Combined Heating System
Sewage source heat pump system cumulative heat supply (kWh)	128,269
Cumulative heat supply of anaerobic reactor biogas boiler system (kWh)	42,500
Total system energy consumption (kWh)	107,557

As can be seen from Figure 8, the energy efficiency ratio of the sewage source heat pump fluctuated around 3.4, while the comprehensive energy efficiency ratio of the combined heating system gradually increased with the increase in the outdoor ambient temperature and solar radiation intensity, and the highest value was 3.08. Because the internal temperature of the anaerobic reactor in the biogas boiler subsystem of the anaerobic reactor in the combined heating system was low in a cold environment, both gas production efficiency and gas production were small, so the amount of heat generated was also small, but the power and power consumption required by the anaerobic reactor during operation were unchanged, so the energy efficiency of the system was relatively low. The anaerobic reactor can have a large gas production efficiency and gas production only at a suitable

temperature, so it is necessary to set up a heating channel for the anaerobic reactor to provide heat for the reactor.The energy efficiency ratio simulation results of the biogas boiler subsystem of the anaerobic reactor under different water supply temperatures are shown in Figure 10.
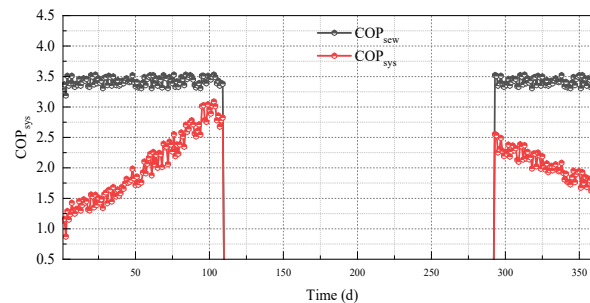

Figure 10. Energy efficiency ratio of combined heating system and heat pump energy efficiency ratio.

5.3. Influence of Water Supply Temperature on the Combined Heating System

The temperature of the water supply is closely related to the efficiency of the heating system, which will directly affect the consumption of energy, and it is necessary to find the most suitable water supply temperature for the specific application to achieve a balance of comfort, energy efficiency, and environmental protection. This section will discuss the performance effects of combined heating systems at different water supply temperatures (45 °C, 50 °C, 55 °C, and 60 °C).

5.3.1. Sewage Source Heat Pump Subsystem

It can be seen that when the water supply temperature of the system increased, the energy efficiency ratio of the sewage source heat pump gradually decreased. When the water supply temperature was 60 °C, the energy efficiency ratio was 3.48 at a minimum; when the water supply temperature was 45 °C, the energy efficiency ratio was 3.74 at the highest, which is consistent with the test data provided by the merchant. Research shows that the lower the water supply temperature of the heat pump unit, the greater the COP value and the better the economy, but when the water supply temperature is too low, the terminal heat dissipation device is too large or unable to meet the internal requirements of the heat dissipation device on the water supply temperature. Therefore, reasonable heat pump water supply temperature is particularly important. Under different water supply temperatures, the comprehensive energy efficiency ratio simulation results of the combined heating system are shown in Figure 11.
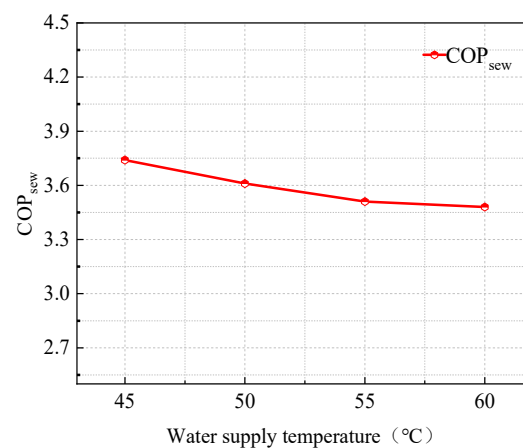

Figure 11. Energy efficiency ratio of sewage source heat pump under different water supply temperatures.

5.3.2. Anaerobic Reactor Biogas Boiler Subsystem

With the increase in the water supply temperature, the energy efficiency ratio of the biogas boiler subsystem of the anaerobic reactor decreased. The maximum energy efficiency ratio was 1.17 when the water supply temperature was 45 °C, and the minimum energy efficiency ratio was 0.88 when the water supply temperature was 60 °C. In order to analyze the reasons for the above phenomena, the heat supply capacities of the sewage source heat pump subsystem and anaerobic reactor biogas boiler subsystem under different water supply temperatures were analyzed, respectively, and the results are shown in Figure 12.
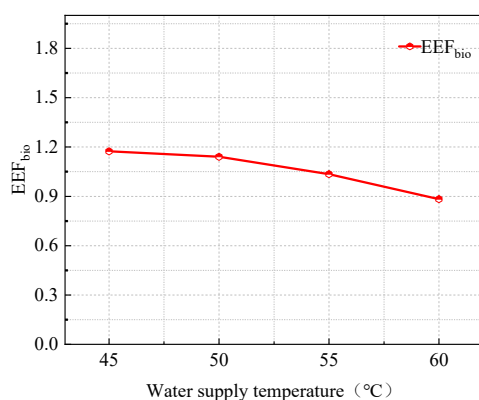

Figure 12. Energy efficiency ratio of biogas boiler subsystem of anaerobic reactor at different water supply temperatures.

5.3.3. The Overall Performance of the System

With the increase in the water supply temperature, the comprehensive energy efficiency ratio of the system decreased continuously. When the water supply temperature was 60 °C, the maximum comprehensive energy efficiency ratio of the system was 2.17, and when the water supply temperature was 45 °C, the minimum comprehensive energy efficiency ratio of the system was 1.79.As can be seen from the figure, with the increase in the water supply temperature, the heat supply capacity of the sewage source heat pump subsystem gradually increased, reaching a maximum value of 131.47 MW·h when the water supply temperature was 60 °C, while the heat supply capacity of the biogas boiler subsystem of the anaerobic reactor gradually decreased, decreasing from 41.082 MW·h when the water supply temperature was 45 °C. It decreased to 30.912 MW·h when the water supply temperature was 60 °C. This was because the gas production of the anaerobic reactor was certain. As the water supply temperature of the combined heating system gradually increased, the temperature difference between the boiler outlet temperature in the biogas boiler subsystem of the anaerobic reactor and the water at the bottom of the hot water collection tank decreased, resulting in the heat in the heat collection tank being unable to be delivered to the heating end in time. Therefore, the heat supply of the sewage source heat pump subsystem increased with the increase in temperature. The heat supply of the biogas boiler subsystem of the anaerobic reactor gradually decreased. Figure 13 shows the energy consumption of the combined heating system under different water supply temperatures. With the increase in water supply temperature, the energy consumption of the combined heating system gradually increased. When the water supply temperature was 45 °C, the energy consumption of the system was 74.88 MW·h; when the water supply temperature was 60 °C, the energy consumption of the system was 90.66 MW·h. Under different anaerobic reactor volumes, the energy efficiency ratio simulation results of the sewage source heat pump subsystem are shown in Figure 14.Under different anaerobic reactor volumes, the energy efficiency ratio simulation results of the biogas boiler subsystem of the anaerobic reactor are shown in Figure 15.
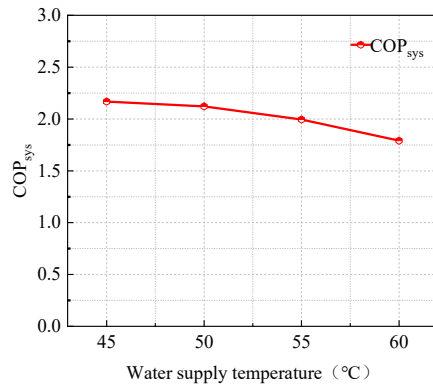
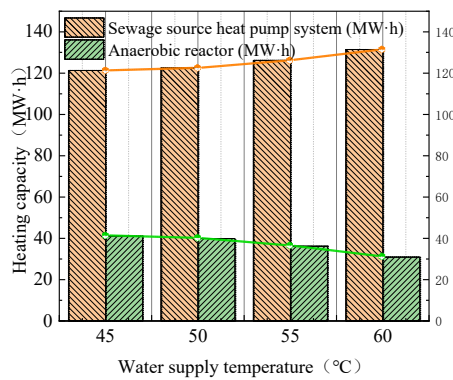**Figure 13.** Comprehensive energy efficiency ratio of the system at different water supply temperatures.

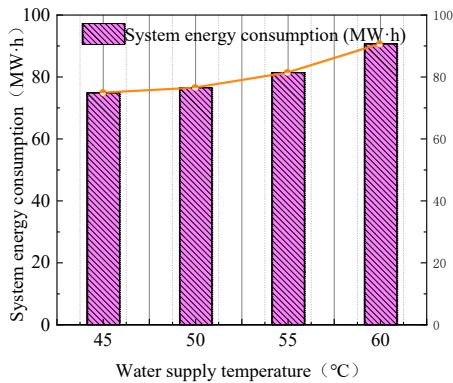**Figure 14.** System heat supply at different water supply temperatures.

Figure 15. System energy consumption at different water supply temperatures.

5.4. Influence of Anaerobic Reactor Volume on Combined Heating System
5.4.1. Sewage Source Heat Pump Subsystem

It can be seen that, with the increase in anaerobic reactor volume, the energy efficiency ratio of the sewage source heat pump gradually decreased. When the anaerobic reactor volume was 45 m^3, the energy efficiency ratio was the minimum of 2.99, and when the anaerobic reactor volume was 30 m^3, the energy efficiency ratio was the highest at 3.48. Under different anaerobic reactor volumes, the system comprehensive energy efficiency ratio simulation results of the combined heating system are shown in Figure 16. With the increase in the anaerobic reactor volume, the overall energy efficiency ratio of the system decreased continuously. When the anaerobic reactor volume was 30 m^3, the maximum energy efficiency ratio of the system was 2.17, and when the anaerobic reactor volume was 45 m^3, the minimum energy efficiency ratio of the system was 1.81. The reasons for the change of

comprehensive energy efficiency ratio and the heat supply of the two subsystems are analyzed below. Figure 17 shows the heat supply of the sewage source heat pump subsystem and the biogas boiler subsystem of the anaerobic reactor under different anaerobic reactor volumes.
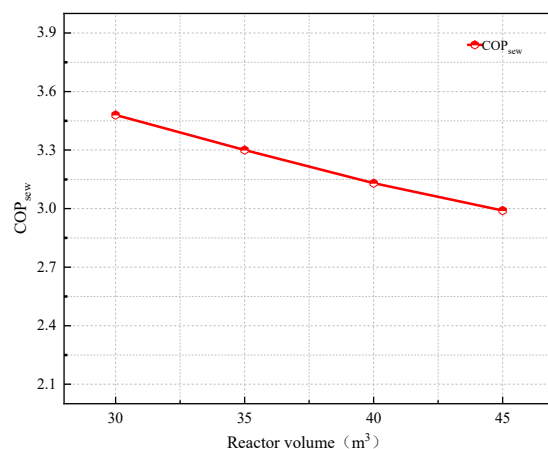

Figure 16. Energy efficiency ratio of sewage source heat pump under different reactor volumes.

5.4.2. Anaerobic Reactor Biogas Boiler Subsystem

With the increase in the anaerobic reactor volume, the energy efficiency ratio of the biogas boiler subsystem of the anaerobic reactor decreased. The maximum energy efficiency ratio was 1.32 when the anaerobic reactor volume was 30 m^3, and the minimum energy efficiency ratio was 1.22 when the anaerobic reactor volume was 45 m^3. This was because as the volume of the anaerobic reactor increased, its power during operation also increased, and the heat required to maintain its constant temperature fermentation gradually increased, so its energy efficiency ratio gradually decreased, but the reduction was not large.
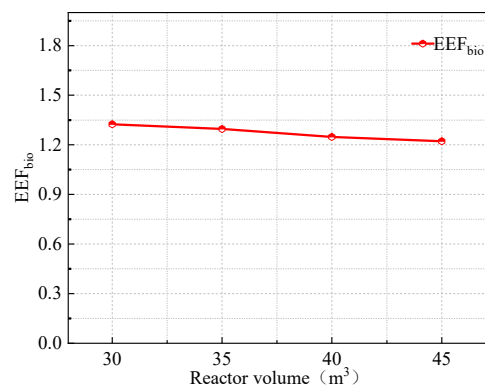

Figure 17. Energy efficiency ratio of biogas boiler subsystem of anaerobic reactor under different reactor volumes.

5.4.3. The Overall Performance of the System

It can be seen from the figure that, with the increase in the anaerobic reactor volume, the heat supply of the sewage source heat pump subsystem gradually decreased. When the anaerobic reactor volume was 30 m^3, the heat supply was 121.3 MW·h, and when the anaerobic reactor volume was 45 m^3, the heat supply of the sewage source heat pump subsystem gradually decreased. The heat supply was 102.61 MW·h. The heat supply of the biogas boiler subsystem of the anaerobic reactor gradually increased. When the volume of the anaerobic reactor was 30 m^3, the heat supply was 41.08 MW·h, and when the volume of the anaerobic reactor was 45 m^3, the heat supply was 61.62 MW·h. This is because, with the increase in the volume of the anaerobic reactor and the increase in gas production,

the heat generated by its combustion also gradually increased, and the building heat load remained unchanged. With the increase in the heat supply of the biogas boiler subsystem of the anaerobic reactor, the heat supply of the sewage source heat pump subsystem decreased accordingly. Figure 18 shows the energy consumption of the combined heating system under different anaerobic reactor volumes. As the volumes of different anaerobic reactors increased, the energy consumption of the combined heating system also increased gradually. As the volume of the anaerobic reactor increased, its power during operation increased, and the heat required to maintain its constant temperature fermentation also increased gradually. The energy consumption generated during operation was greater than the heat provided by the increase in gas production. When the anaerobic reactor volume was 30 m^3, the system's energy consumption was 74.88 MW·h, and when the anaerobic reactor volume was 45 m^3, the system's energy consumption was 89.76 MW·h, as shown in Figures 19 and 20.
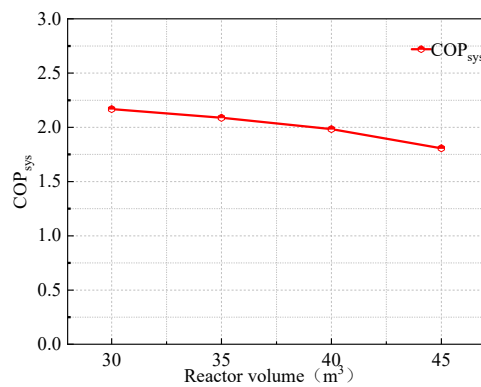

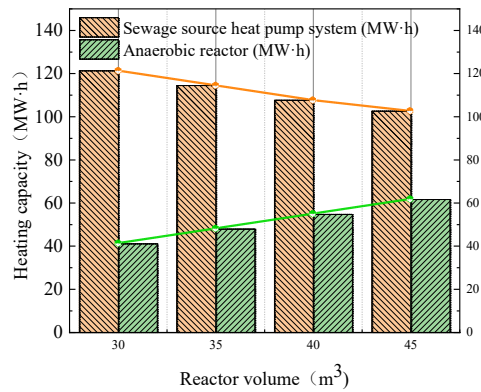**Figure 18.** Comprehensive energy efficiency ratio of the system under different reactor volumes.

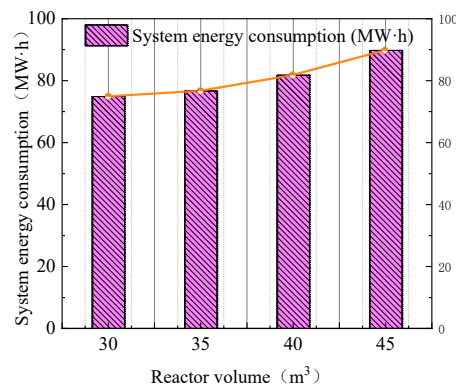**Figure 19.** Heating capacity of the system under different reactor volumes.

Figure 20. System energy consumption under different reactor volumes.

5.5. Economic Benefit Analysis

The traditional coal-fired heating system and multi-energy complementary combined heating system are analyzed, respectively. The initial investment of the main equipment of the heating system is shown in the table below, without considering the costs incurred during the installation process [22].

5.5.1. Initial System Investment

The investment for each heating system is shown in Tables 6 and 7:

Table 6. Initial investment costs of multi-energy complementary combined heating systems.

Device Name	Quantity	Price (CNY)
Sewage source heat pump unit	1	50,000
Heat exchanger	1	5000
Direct absorption solar anaerobic reactor	1	70,000
Biogas boiler	1	9800
Circulating water pump	6	3600
Control system	controller	1500
cistern	1	7500
total		153,400

Table 7. Initial investment costs for traditional coal-fired heating systems.

Device Name	Quantity	Price (CNY)
Coal-fired boiler	1	20,000
Circulating water pump	1	600
Control system	controller	1500
cistern	1	7500
total		29,600

From the initial investment shown in Tables 6 and 7, it can be seen that the initial investment cost of the multi-energy complementary combined heating system was CNY 153,400, while the initial investment cost of the traditional coal-fired heating system was CNY 29,600 Yuan. The initial investment cost of the multi-energy complementary combined heating system was 418.2% higher than that of the traditional coal-fired heating system. This is mainly because of the high cost of equipment in the new combined heating system, which is one of the important reasons hindering the development of the multi-energy complementary combined heating system at present, but the cost generated in operation has a greater advantage compared with the traditional heating system, and the combined heating system has good environmental benefits, so it has a good application prospect.

5.5.2. Annual System Operating Cost

The energy consumption of the multi-energy complementary combined heating system is mainly electric energy, and the electricity is priced according to the electricity price of 0.5 CNY/kWh. The operating cost of the multi-energy complementary combined heating system is shown in Table 8 below, which simulates the entire heating season from 1 January to 20 April and from 20 October to 31 December in a year:

Table 8. Price of electricity.

Mode of Operation		Energy Consumption	Quantity (kWh)	Unit Price of Energy	Total Annual Cost (CNY)
Conventional coal-fired heating		Coal + Electricity	24t/3064	1400 Yuan/t	35,132
Multi-energy complementary combined heating	unheated	Electric energy	107,556	0.5 Yuan/kWh	53,778
	33 °C	Electric energy	69,288	0.5 Yuan/kWh	34,644
	35 °C	Electric energy	55,296	0.5 Yuan/kWh	27,648
	37 °C	Electric energy	69,373	0.5 Yuan/kWh	34,686.5

As can be seen from Table 8, the anaerobic reactor in the biogas boiler subsystem of the multi-energy complementary combined heating system has the highest energy consumption under the condition of no heating, and its total annual operating cost is also the highest, which is CNY 18,646 higher than that of the traditional coal-fired heating system. The reason is that at this time, the operation of the anaerobic reactor leads to significant energy consumption, but the heat supply provided by the biogas combustion is small, and the total energy consumption of the system is the maximum at this time. When the temperature of the anaerobic reactor is maintained at 35 °C, the gas production of the anaerobic reactor is the highest, and the heat load borne by the gas-producing combustion is far greater than the energy consumption generated by temperature maintenance. At this time, the total energy consumption of the system is the lowest, and the total annual operating cost is also the lowest. The average coal consumption per ton is CNY 1400, the overall cost of traditional coal-fired heating is CNY 35,132, and the overall cost of using a sewage source heat pump alone is CNY 53,778. The cost of using a direct suction anaerobic reactor and a sewage source heat pump for simultaneous heating at 37 °C is CNY 34,686.5. Finally, the total cost of this hybrid heating system at 35 °C is CNY 27,648. Compared with traditional coal-fired power plants, this system can save CNY 7484, with an investment of CNY 35,450 and a recovery cycle of approximately 4.7 years.

5.5.3. Annual System Cost

In this study, the designed service life of the equipment in the new combined heating system is 15 years, and the annual cost of the system is calculated. The annual cost is calculated in Table 9.

Table 9. Annual values of system costs.

Mode of Operation	Conventional Coal-Fired Heating	New Waste Heat and Biogas Combined Heating			
---	---	unheated	33 °C	35 °C	37 °C
Annual cost	53,496	72,742.5	53,608	46,612	53,650

The calculated present value of the cost of the multi-energy complementary combined heating system is only CNY 46,612 when the reactor temperature is maintained at 35 °C, which is CNY 26,130.5 less than that without the reactor heating channel, and the annual costs are CNY 53,608 and CNY 53,650 when the reactor temperature is maintained at 33 °C and 37 °C, respectively. The annual cost of the traditional coal-fired heating system is CNY 53,496. It can be seen that, from an economic point of view, the combined heating system with a reactor heating channel is far better than the multi-energy complementary combined heating system without a reactor heating channel.

5.5.4. Environmental Benefit Analysis

According to the environmental benefit evaluation index, the environmental benefit parameters under different heating schemes are calculated in Table 10.

Table 10. Results of environmental benefit assessment.

Item	Multi-Energy Complementary Combined Heating			
Temperature (°C)	unheated	33	35	37
System Energy consumption (kWh)	107,556	69,288	55,296	69,373
Carbon dioxide emission reduction (t)	9.15	11.35	12.15	11.23
Sulfur dioxide emission reduction (kg)	74.1	91.9	98.4	90.2
Dust reduction (kg)	37.1	46.2	49.2	45.5
Annual treatable sewage (t)	2700	2700	2700	2700

As can be seen from Tables 5 and 6, the anaerobic reactor in the multi-energy complementary combined heating system can reduce carbon emissions by 12.15 t, sulfur dioxide by 98.4 kg, and dust emissions by 49.2 kg per year under the condition of maintaining 35 °C, which has obvious effects on energy saving and environmental protection. Through the analysis of the energy efficiency, economic benefits, and environmental benefits of the multi-energy complementary joint heating system, it can be seen that maintaining the fermentation temperature of the reactor at 35 °C leads to significant environmental protection compared with maintaining the reactor heating channel at 33 °C and 37 °C. In addition, the annual sewage treatment capacity of the multi-energy complementary combined heating system can reach 2700 tons, which means that the system can not only use energy efficiently, but also treat sewage, reducing the adverse impact on the environment.

6. Conclusions and Prospects

In this paper, a multi-energy complementary combined heating system suitable for oilfield areas is proposed based on the current efficient treatment and utilization of oilfield sewage. A typical dormitory apartment building in oil area is selected as the research object, and the building heat load is output by DeST. The mathematical model and evaluation index of each component of the system are established, the operating characteristics and influencing factors of the system on typical days and in typical heating seasons are analyzed based on TRNSYS software, and the economic and environmental benefits of the system are simulated and calculated. The main conclusions of this study are as follows:

(1) Through a simulation study of the system on two typical days and in a typical heating season, the results show that, under the simulated conditions of two typical days and the typical heating season, the main heating heat load is borne by the sewage source heat pump, the energy efficiency of the system is lower than that in cold conditions, and the energy-saving characteristics are not obvious.

(2) The combined heating system maintains the heat demand of the reactor at different fermentation temperatures, the energy supply and energy consumption of the combined heating system, and the energy efficiency ratio of each system. The results show that, under the condition of maintaining the fermentation temperature of the anaerobic reactor at a constant temperature of 35 °C, the energy efficiency ratio and energy consumption of the system are the best.

(3) The effects of the heating temperature and anaerobic reactor volume on the combined heating system were studied. The results show that, with the increase in the heating temperature and anaerobic reactor volume, the system energy consumption increases, and the system energy efficiency ratio decreases gradually.

(4) The economic and environmental benefits of the multi-energy complementary combined heating system are analyzed. The results show that the economy of the combined heating system is the best under the condition of maintaining a constant temperature of 35 °C. Although the initial investment of the combined heating system is high, its operating cost and environmental benefits are huge. Under the condition of maintaining a temperature of 35 °C, the anaerobic reactor in the multi-energy complementary joint heating system can reduce carbon emissions by 12.15 t per year, reduce sulfur dioxide by 98.4 kg, reduce dust emissions by 49.2 kg, and treat up to 2700 t of sewage per year, which has broad application prospects.

(5) According to a comparison of experimental data with simulation data, the error value of the supply and return water temperature of the sewage source heat pump unit is only 0.75%. Therefore, using this model can ensure the reliability and accuracy of the simulation results, and can be used for modeling and analysis of mixed heating systems.

In addition, based on the above research, the following work can be carried out in the future:

(1) The gas production of the biogas boiler subsystem of the anaerobic reactor is idealized in the TRNSYS model, which ignores the influence of the reaction substrate and other factors. The actual gas production may be deviated from the reactor. In the future, the actual situation should be considered in the actual application process to adjust the gas production.

(2) The sewage source heat pump heating system is selected in the TRNSYS model verification process, and the model verification process of the combined heating system is lacking. In the future, small device test stands can be arranged or similar projects can be sought to collect the measured data of the combined heating system, so as to better complete the model verification work.

Author Contributions: M.X. is mainly responsible for simulating the system in the artcile, Z.X. is mainly responsible for building the model, X.W., G.Z. and C.L. are mainly responsible for data processing in the later stage. All authors have read and agreed to the published version of the manuscript.

Institutional Review Board Statement: Exclude this statement.

Informed Consent Statement: Not applicable.

Data Availability Statement: The data that support the findings of this study are available from the corresponding author upon reasonable request.

Conflicts of Interest: The authors declare no conflict of interest.

Nomenclature

Symbols		Subscripts	
T	Temperature	*iar*	Inside the anaerobic reactor
k_p	The drag coefficient	*ref*	Optimum fermentation temperature in anaerobic reactor
Pa	Pressure	*anr*	The average value of the mixture in the anaerobic reactor
q	Heat	*g*	Ground
R_{bg}	Calorific value of methane	*Bb*	Biogas boiler
v	volume	*af, i*	Anaerobic reactor feed material
m	Mass flow	*h, l*	High temperature measurement and low temperature measurement
p	Power	*ar*	anaerobic reactor
U	Tank heat transfer coefficient	*gas*	Gases in an anaerobic reactor
A	Heat transfer area of the tank	*a*	atmosphere
e	The value of electricity consumption converted to primary energy	*he*	Heat exchanger
Q	The total amount of wastewater treated	*sew*	Wastewater source heat pump
N	Load rate	*ab*	Absorb
C	COD concentration	*TR*	Tradition
Greek letters		*u*	Unit
η	Thermal efficiency	*meth*	Methane

References

1. Chang, S.; Hatef, M.; Björn, P. Heating solutions for residential buildings in China: Current status and future outlook. *Energy Convers. Manag.* **2018**, *177*, 493–510.
2. Lei, L.; Ilhan, O.; Muntasir, M. Environmental innovations, energy innovations, governance, and environmental sustainability: Evidence from South and Southeast Asian countries. *Resour. Policy* **2023**, *82*, 103556. [CrossRef]
3. Chang, S.; Hatef, M.; Björn, P. Building heating solutions in China: A spatial techno-economic and environmental analysis. *Energy Convers. Manag.* **2019**, *179*, 201–218.
4. Huan, Y.Z.; Ma, L.S.; Zhi, Y.S. The evolution of renewable energy and its impact on carbon reduction in China. *Energy* **2021**, *237*, 121639.
5. María, V.J.; Estrella, T. Discontinuity in the production rate due to the solar resource intermittency. *J. Clean. Prod.* **2021**, *321*, 128976.
6. Tai, L.L.; Jia, L.Z.; Shou, L.X. A novel geothermal system combined power generation, gathering heat tracing, heating/domestic hot water and oil recovery in an oilfield. *Geothermics* **2014**, *51*, 388–396.
7. Yao, W.C.; Meng, M.G.; Yan, F.L. Energy, exergy, and economic analysis of a centralized solar and biogas hybrid heating system for rural areas. *Energy Convers Manag.* **2023**, *276*, 116591.
8. Ji, B.L.; Kui, M.X.; Hui, H.Z. Study on energy-saving operation of a combined heating system of solar hot water and air source heat pump. *Energy Convers. Manag.* **2021**, *229*, 113624.
9. Yang, W.; Sun, L.; Chen, Y. Experimental investigations of the performance of a solar-ground source heat pump system operated in heating modes. *Energy Build.* **2015**, *89*, 97–111. [CrossRef]
10. Ioan, S.; Calin, S. General review of ground-source heat pump systems for heating and cooling of buildings. *Energy Build.* **2014**, *70*, 441–454.
11. Yu, B.W.; Zhen, H.Q.; Yao, H.Z. Operation mode performance and optimization of a novel coupled air and ground source heat pump system with energy storage: Case study of a hotel building. *Renew. Energy* **2022**, *201 Pt 1*, 889–903.
12. Cong, G.H.; Jia, M.S.; Martin, L. Design and simulation of a novel hybrid solar-biomass energy supply system in northwest China. *J. Clean. Prod.* **2019**, *233*, 1221–1239.
13. Shah, M.; Vaidya, D.; Dhale, S. Exploitation and Utilization of Oilfield Geothermal Resources in INDIA. In *Nanotechnology for Energy and Water*; Anand, G., Pandey, J., Rana, S., Eds.; Springer: Cham, Switzerland, 2018; Volume 128, pp. 47–54.
14. Chatzistougianni, N.; Giagozoglou, E.; Sentzas, K. Biomass district heating methodology and pilot installations for public buildings groups. *IOP Conf. Ser. Mater. Sci. Eng.* **2016**, *161*, 012083. [CrossRef]
15. Yan, L.; Yan, F.L.; Zhao, S.Y. The investigation of co-combustion of sewage sludge and oil shale using thermogravimetric analysis. *Thermochim. Acta* **2017**, *653*, 71–78.
16. Jun, P.H.; Jia, N.F.; Simon, F. Feasibility study on solar district heating in China. *Renew. Sustain. Energy Rev.* **2019**, *108*, 53–64.
17. Shi, Y.Y.; Qiang, W. New progress and prospect of oilfields development technologies in China. *Petrol. Explor. Dev* **2018**, *45*, 698–711.
18. Kai, W.; Bin, Y.; Guo, M.J. A comprehensive review of geothermal energy extraction and utilization in oilfields. *J. Petrol. Sci. Eng.* **2018**, *168*, 465–477.
19. Cui, P.L.; Chuang, Z.W.; Yan, Y.J. Chemical elemental characteristics of biomass fuels in China. *Biomass Bioenergy* **2004**, *27*, 119–130.
20. Jie, L.J.; Fen, C.; Shuai, L.; Ying, W.Y.; Chang, J.H.; Yong, Z.W. Co-production of biogas and humic acid using rice straw and pig manure as substrates through solid-state anaerobic fermentation and subsequent aerobic composting. *J. Environ. Manag.* **2022**, *320*, 115860. [CrossRef]
21. Pater, S. Long-Term Performance Analysis Using TRNSYS Software of Hybrid Systems with PV-T. *Energies* **2021**, *14*, 6921. [CrossRef]
22. Myszograj, S.; Bocheński, D.; Mąkowski, M.; Płuciennik-Koropczuk, E. Biogas, Solar and Geothermal Energy—The Way to a Net-Zero Energy Wastewater Treatment Plant—A Case Study. *Energies* **2021**, *14*, 6898. [CrossRef]
23. Abdulkarim, A.; Faruk, N.; Alozie, E.; Olagunju, H.; Aliyu, R.Y.; Imoize, A.L.; Adewole, K.S.; Imam-Fulani, Y.O.; Garba, S.; Baba, B.A.; et al. Advances in the Design of Renewable Energy Power Supply for Rural Health Clinics, Case Studies, and Future Directions. *Clean Technol.* **2024**, *6*, 921–953. [CrossRef]
24. Stamatellos, G.; Zogou, O.; Stamatelos, A. Energy Performance Optimization of a House with Grid-Connected Rooftop PV Installation and Air Source Heat Pump. *Energies* **2021**, *14*, 740. [CrossRef]
25. Krarouch, M.; Lamghari, S.; Hamdi, H.; Outzourhit, A. Simulation and experimental investigation of a combined solar thermal and biomass heating system in Morocco. *Energy Rep.* **2020**, *6*, 188–194. [CrossRef]
26. Jiang, J.W.; Chao, F.M.; Jing, W. Thermodynamic analysis of a combined cooling, heating and power system based on solar thermal biomass gasification. *Appl. Energy* **2019**, *247*, 102–115.
27. Magdi, R.; Alina, Ż.-G.; Les, N. Analysis of energy demand in a residential building using TRNSYS. *Energy* **2022**, *254*, 124357.
28. Ahamed, M.S.; Guo, H.; Tanino, K. Modeling heating demands in a Chinese-style solar greenhouse using the transient building energy simulation model TRNSYS. *J. Build. Eng.* **2020**, *29*, 101114. [CrossRef]
29. Li, H.; Sun, L.; Zhang, Y. Performance investigation of a combined solar thermal heat pump heating system. *Appl. Therm. Eng.* **2014**, *71*, 460–468. [CrossRef]

30. Deng, J.W.; Ran, C.; Yong, Z.Y. Optimization and techno-economic analysis of combined gas-fired boiler and solar heating system for capacity-increase cities. *Sol. Energy* **2022**, *243*, 225–235.
31. Fatemeh, B.; Khosrow, R. Application of kinetic models in dark fermentative hydrogen production—A critical review. *Int. J. Hydrogen Energy* **2022**, *47*, 21952–21968.
32. Zhou, H.; Ying, Z.; Cao, Z. Feeding control of anaerobic co-digestion of waste activated sludge and corn silage performed by rule-based PID control with ADM1. *Waste Manag.* **2020**, *103*, 22–31. [CrossRef] [PubMed]
33. Ming, Z.J.; Guo, H.F.; Kai, L.H. Research and Analysis of Combined Operational Mode of Solar Energy Hot Water Heating System and Sewage Source Heat Pump Units. *Procedia Eng.* **2015**, *121*, 1544–1555.
34. Tian, T.Z.; Yu, F.T.; Xue, D.Z. Using a hybrid heating system to increase the biogas production of household digesters in cold areas of China: An experimental study. *Appl. Therm. Eng.* **2016**, *103*, 1299–1311.